



In silico investigation of saponins and tannins as potential inhibitors of SARS-CoV-2 main protease (M^{pro})

Victoria Adeola Falade¹ · Temitope Isaac Adelusi³ · Ibrahim Olaide Adedotun² · Misbaudeen Abdul-Hammed² · Teslim Alabi Lawal² · Saheed Alabi Agboluaje⁴

Received: 14 October 2020 / Accepted: 18 December 2020
© The Author(s), under exclusive licence to Springer-Verlag GmbH, DE part of Springer Nature 2021

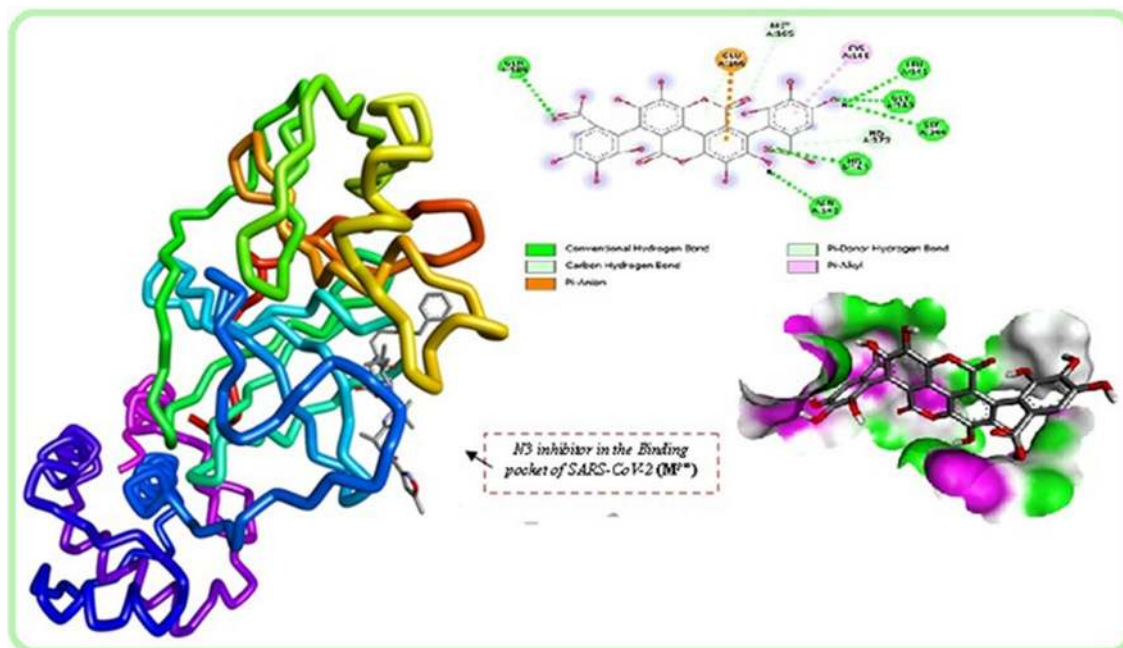
Abstract

It is no longer news that a novel strain of coronavirus named SARS-CoV-2 is ravaging the health sector worldwide, several attempts have been made to curtail this pandemic via repurposing of old drugs but at the present, available drugs are not adequately effective. Over the years, plant phytochemicals are increasingly becoming alternative sources of antimicrobial agents with novel mechanisms of action and limited side effects compared to synthetic drugs. Isolated saponins and tannins were evaluated for antiviral activity against SARS-CoV-2 (M^{pro}) via Molecular Docking and it was observed that a handsome number of the phytochemicals had binding affinities much better than Remdesivir, Dexamethasone, and N3 inhibitor which were used as the standards in this study. Further investigation of drug-likeness, ADMET profile, PASS profile, oral bioavailability, bioactivity, binding mode, and molecular interactions of these phytochemicals revealed that binding affinity alone is not enough to justify the potency of a molecule in the drug discovery process, as only 4 among the screened compounds passed all the analyses and are identified as potential inhibitors of SARS-CoV-2 (M^{pro}). This preliminary study thereby recommends Ellagic acid (− 8.4 kcal/mol), Arjunic Acid (− 8.1 kcal/mol), Theasapogenol B (− 8.1 kcal/mol), and Euscaphic Acid (− 8.0 kcal/mol) as potential inhibitors of SARS-CoV-2 (M^{pro}) with better pharmacokinetics and bioavailability compared to Remdesivir which is currently used compassionately.

✉ Misbaudeen Abdul-Hammed
mabdul-hammed@lautech.edu.ng

- ¹ Organic Chemistry Unit, Department of Pure and Applied Chemistry, Ladoke Akintola University of Technology, Ogbomoso, Oyo State, Nigeria
- ² Biophysical and Computational Chemistry Unit, Department of Pure and Applied Chemistry, Ladoke Akintola University of Technology, Ogbomoso, Oyo State, Nigeria
- ³ Computational Biology/Drug Discovery Laboratory, Department of Biochemistry, Ladoke Akintola University of Technology, PMB 4000, Ogbomoso, Nigeria
- ⁴ Department of Chemistry, Ekiti State University, Ado Ekiti, Ekiti State, Nigeria

Graphic abstract



Keywords Molecular docking · Saponins · Tannins · Pharmacokinetics · Drug-likeness · SARS-CoV-2 (M^{Pro})

Introduction

The outbreak of a novel strain of coronavirus has been an unprecedented challenge in the healthcare system globally. This was initially identified in a cluster of Pneumonia patients in Wuhan, Hubei province, China in December 2019 and had since spread to other continents of the world (Zhou et al. 2020; Chang et al. 2020). The causative virus was found to be closely related to a previously known Severe Acute Respiratory Syndrome Coronavirus (SARS-CoV), hence the name SARS-CoV-2 (Wand et al. 2020). Clinical symptoms include pneumonia, cold, dry cough, sore throat, fever, shortness of breath, respiratory tract infection, headache, diarrhea, and abdominal pain (Chen et al. 2020). Over twenty (20) million symptomatic and asymptomatic cases had been reported, with more than a million deaths (<https://coronavirus.jhu.edu/map.html>). The infection was reported to be severe in elderly patients and more critical in individuals with underlying health conditions like diabetics, cardiovascular disease, obesity, pulmonary fibrosis, asthma, cancer, etc (Wu et al. 2020).

As of the time of this report, no drug/vaccine has been proven to effectively cure/manage this infection. The current strategy in the management includes early diagnosis, isolation of infected individuals, and maintenance of personal hygiene, physical distance, and use of personal protective

equipment. Attempts have also been made to reposition/repurpose old drugs of promising antiviral potential in a bid to tackle this fast-spreading pandemic. Remdesivir, lopinavir-ritonavir, favipiravir, etc. are among the drugs used in the management of this pandemic (Wu et al. 2020). More recently dexamethasone has been found to reduce mortality in severe cases of COVID-19 disease (Johnson and Vinetz 2020).

Phytochemicals are increasingly becoming the alternative therapeutic and pharmacological agent of great importance in drug discovery and development. They have limited or no side effects on administration, possess a novel mechanism of action, and great chemical diversity which enhances their therapeutic interaction with varied biological targets compared to synthetic drugs. Saponins are naturally occurring non-volatile and surface-active glycosides of triterpenes and steroids with a wide range of pharmacological activities, including anti-inflammatory, anticancer, antiviral, antitumor, antifungal, hypoglycemic, and cytotoxic activity. They are potential vaccine adjuvant due to their ability to stimulate and activate the immune system in mammals (Sun et al. 2009; Skene and Sutton 2006). The sugar side chain in saponins could be responsible for their adjuvant. Similarly, saponins have been found to possess a novel mechanism of action on the virus which involves the destruction of viral envelop, loss of binding sites, and subsequent prevention of

binding of the virus to host cell (Roner et al. 2007). They have also found application in food, confectionery, beverages, cosmetics, preparation of pharmaceutical products, as well as industrial processes as surface-active and foaming agents. Rich sources of saponins include soya beans, capsicum peppers, spinach, horse chestnut, fenugreek, ginseng, etc. (Francis et al. 2002; Vincken 2007). Moreover, much toxicity is observed when saponins are administered intravenously while lower toxicity is observed when is administered orally due to low absorption in the alimentary canal but it is rather hydrolyzed to sapogenins via enzymatic action (Guclu-Ustundag and Mazza 2007).

Tannins on the other hand are phenolic compounds of great antioxidant potential and antiviral properties, they are high molecular weight compounds (ranging between 500 and 3000 gmol⁻¹) found in different parts of plants including leaf, stem, root, or bark (Serrano et al. 2009). This study aims at investigating the antiviral potential of saponins and tannins against SARS-CoV-2 M^{Pro} through molecular docking coupled with ADMET-studies, pharmacokinetic evaluation, drug likeliness among other analyses at a therapeutic dose.

Methods

Ligands preparation

In this research, the inhibitory activities of twenty-seven (27) phytochemicals from Saponins and Tannins against SARS-CoV-2 main protease (M^{Pro}) PDB ID: 6LU7 were studied. The selected isolated phytochemicals from different species of plants have been reported to possess broad-spectrum biological activities including antiviral, anti-inflammatory, cytotoxic activities, anti-diabetic, neuroprotective, immunomodulatory, antioxidant, and anticancer, to mention a few. Their reported biological activities arouse our interest to investigate them as potential inhibitors of the novel SARS-CoV-2 main protease (M^{Pro}) towards designing a new therapeutic agent. The sources, species name, and biological activities of the studied compounds are shown in Table 1. Also, three standards (Remdesivir, Dexamethasone, and N3 inhibitor) whose completed randomized trials and inhibitory activities against the novel SARS-CoV-2 (M^{Pro}) have been reported (Kaddoura et al. 2020; Jin et al. 2020) were used for comparison. The Saponins/Tannins used are Priverogenin A, Arjunic acid, Theasapogenol B, Euscaphic Acid, Camelliagenin C, Medicagenic Acid, Protoescigenin, Arjunolic acid, Asiatic acid, Protobassic acid, Arjugenin, Polygalic acid, Primulagenin A, Soyasapogenol B, Tomentosic acid, Presenegenin, Punicalagin, Punicalin, Ellagic acid, Corilagin, Gallagic acid, Terflavin B. Catechin, Chebulinic

acid, Hexahydroxydiphenic acid, Gallic acid, and Catechol respectively.

Using conformer distribution with Molecular mechanics/MMFF in Spartan 14 version 1.1.4, the most stable conformers of all the studied compounds were obtained. The conformers were optimized using equilibrium geometry density functional theory method (DFT) at B3LYP and 6 – 31 + G* as the basis set on HP Desktop computer, 2 terabytes hard disk, 64-gigabyte random accessed memory (RAM), Intel® Core™i7-2600 CPU, 3.40 GHz processor, and 4 gigabytes dedicated video memory to generate important molecular properties and well optimized structures for molecular docking simulation.

Preparation of target receptor

The crystal structure of SARS-CoV-2 M^{Pro} (PDB ID: 6LU7) (Fig. 1) was used as a target receptor in this study. The structure was retrieved from the protein data bank (RCSB) (<http://www.rcsb.org/pdb>). SARS-CoV-2 M^{Pro} is the main protease of the novel strain of the 2019 coronavirus disease. It is a protein that mediates replication and transcription of the virus (Jin et al. 2020), therefore, the protease is often the target of the potential inhibitors of the virus in the drug discovery and development processes. The resolution of 6LU7 (2.16 Å) approximately falls within the 2.0 Å recommended resolution for a protein of good quality (Hajduk and Tse 2005). Water molecules and other unwanted complexes were removed from the downloaded protease to avoid undesired molecular interactions and to ensure that no molecule interfered with the potential binding site of the target protease during the docking simulation. The Ramachandran plot (Fig. 2) which revealed the quality of the receptor under study was obtained using the Volume, Area, Dihedral Angle Reporter (VADAR) webserver. The binding pocket X, Y, and Z coordinates were defined as – 26.284, 12.603, and 58.96 respectively for the screening exercise using the grid box of the native ligand inhibitor (N3 inhibitor) complexed with the target receptor as a basis.

Determination of (6LU7) M^{Pro} active sites

Binding pocket, ligand interactions, and all amino acids in the active site of SARS-CoV-2 M^{Pro} were established using the Computed Atlas for Surface Topography of Proteins (CASTp) (<http://sts.bioe.uic.edu/castp/index.html?2011>) (Tian et al. 2019) and Biovia Discovery Studio (2019). The obtained data were compared and validated with the previously reported experimental data for the SARS-CoV-2 M^{Pro} active site complexed with N3 native ligand (Jin et al. 2020).

Table 1 Source of studied ligands and their biological activities

Ligand	Species name	Biological activities/References
Priverogenin A	<i>Thea sinensis</i>	Cytotoxic activity (Thakur et al. 2011)
Arjunic acid	<i>Terminalia arjuna</i>	Anticancer (Saxena et al. 2007); antioxidant (Pawar and Bhutani 2005)
Theasapogenol B	<i>Camellia sasanqua</i> <i>Aesculus, Stryax,</i> <i>Camellia, Barringtonia</i>	Anti-inflammatory, hepatoprotective, Anti cancer, insecticidal, molluscidal, antimicrobial, antioxidant (Chen et al. 2010b, 2015; Liu et al. 2007, 2014; Zhao et al. 2015; Yang et al. 2015; Kaprayoon et al. 2014; Kim et al. 2015; Li et al. 2014)
Euscaphic Acid	<i>Folium Eriobotryae</i> <i>Geum japonicum</i> <i>Rosa rugosa</i>	Anti-diabetic (Chen et al. 2008) Antiviral (Hong-Xi Xu et al. 1996) Anti-inflammatory (Kim et al. 2012)
Camelliagenin C	<i>Camellia Oleifera</i>	Antibacterial (Ye et al. 2015)
Medicagenic Acid	<i>Medicago sativa</i>	Hemolytic activities (Oleszek et al.)
Protoescigenin	<i>Aesculus hippocastanum</i>	Parkes Weber syndrome treatment (Zhang et al.)
Arjunolic acid	<i>Terminalia arjuna</i>	Antilipidemic, antiinflammatory, antioxidant, and immunomodulatory properties (Gosh and Sil 2013)
Asiatic acid	<i>Centella asiatica</i>	Neuroprotective activity (Lee et al. 2000)
Protobassic acid	<i>Madhuca indica</i>	Antioxidant (Pawar and Buthani 2004)
Arjungenin	<i>Terminalia arjuna</i>	Antilipidemic, antiinflammatory, antioxidant, and immunomodulatory properties (Gosh and Sil 2013). (Row 1962)
Polygalacic acid	<i>Polygala,</i> <i>Solidago</i>	Antifungi (Based et al. 2000)
Primulagenin A	<i>Primula eliator</i> <i>Jacquinia</i>	Cytotoxic activity (Podolak et al. 2010)
Soyasapogenol B	<i>Glycine max</i>	Antiviral (HSV-1) activity (Ikeda et al. 2005)
Tomentosic acid	<i>Bixa orellana</i>	Anti-inflammatory, antitumour, antioxidant, antibacterial (Lourido and Martinez 2010)
Presenegenin	<i>Securidaca longipedunculata</i>	Antiparasitic, Antibacterial (Fernandez et al. 2008; Junaid et al. 2008)
Punicalagin	<i>Prunica granatum</i>	Antioxidant, Anti-inflammatory, Antiproliferative Hepatoprotective, Antigenotoxic, Anticancer properties (Lin et al. 1999; 2001; Chen et al. 2000; Landete 2011; Seram et al. 2005; Heber 2008)
Punicalin	<i>Prunica granatum,</i> <i>Terminalia catappa</i>	Antioxidant, Anti-atherogenic (Kaplan et al. 2001; Khateeb et al. 2010), Antimicrobial, Anti-inflammatory, Anticancer properties (Lee et al. 2006; Na et al. 2006; Ngoumfo et al. 2008; Toronen 2009)
Ellagic acid	<i>Prunica granatum</i>	Antioxidant, Anti-inflammatory, Antiproliferative, Hepatoprotective, Antigenotoxic, Anticancer properties (Lin et al. 1999; 2001; Chen et al. 2000; Landete 2011; Seram et al. 2005; Heber 2008)
Corilagin	<i>Phyllanthus niruri</i>	Antiatherogenic, Antioxidant, Hepatoprotective Antitumor (Duan et al. 2005; Chen and Chen 2011; Kinoshita et al. 2007; Hau et al. 2010)
Gallagic acid	<i>Prunica granatum</i>	Antioxidant, Anti-atherogenic (Kaplan et al. 2001; Khateeb et al. 2010) Antimicrobial, Anti-inflammatory, Anticancer properties (Lee et al. 2006; Na et al. 2006; Ngoumfo et al. 2008; Toronen 2009)
Terflavin B	<i>Terminalia catappa</i> <i>Myrobalanus chebula</i> <i>Terminalia chebula</i>	Antibacterial, Antiviral activity (Rathinamoorthy and Thilagavathi 2014; Lee et al. 2011)
Catechin	<i>Camellia sinensis</i>	Ant-inflammatory, Antioxidative Immune and epigenetic modification, Inhibition of tyrosine kinase receptor (Shirakami and Shimzu 2018)
Chebulinic acid	<i>Terminalia chebula</i>	Antibacterial, Antiviral activity (Rathinamoorthy and Thilagavathi, 2014; Lee et al. 2011)
Hexahydroxydiphenic acid	<i>Prunica granatum</i>	Antioxidant, Anti-atherogenic (Kaplan et al. 2001; Khateeb et al. 2010) Antimicrobial, Anti-inflammatory Anticancer properties (Lee et al. 2006; Na et al. 2006; Ngoumfo et al. 2008; Toronen 2009)
Gallic acid	<i>Terminalia chebula</i>	Antibacterial, Antiviral activity (Rathinamoorthy and Thilagavathi 2014; Lee et al. 2011)
Catechol	<i>Acacia nilotica</i>	Antioxidant (Amos et al. 1999)

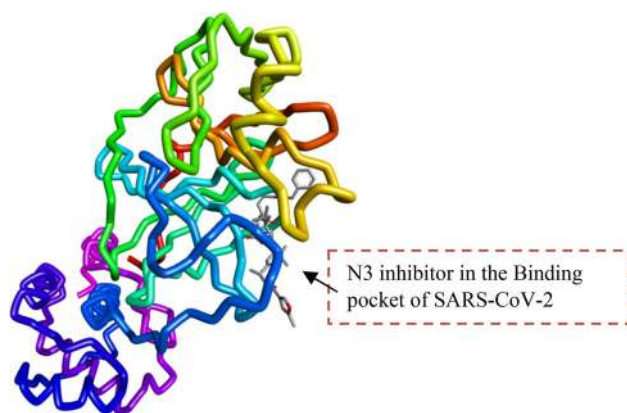
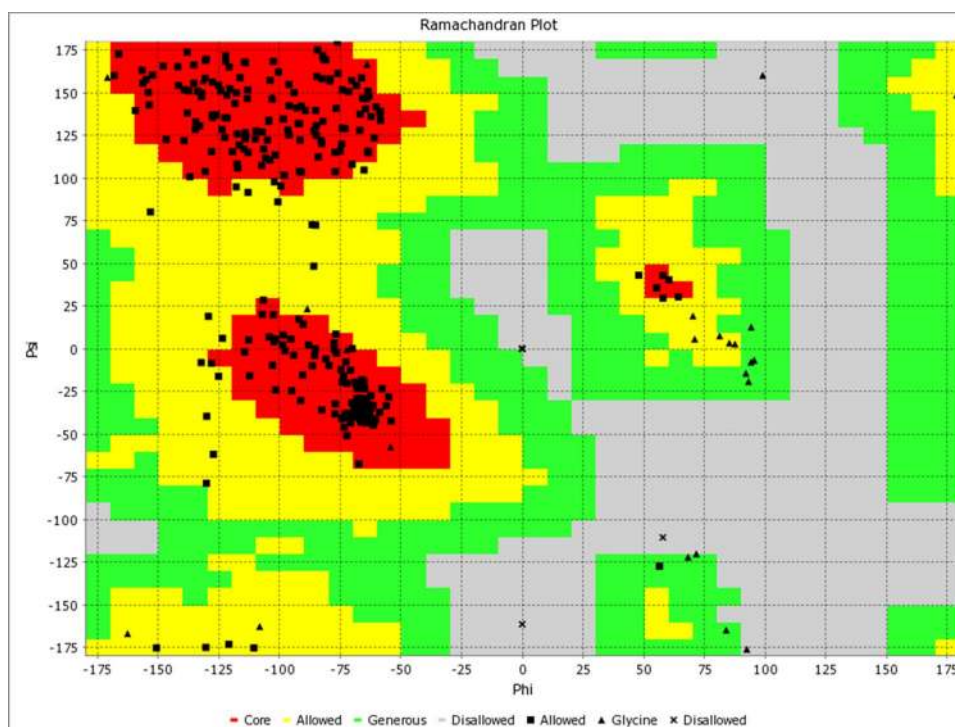


Fig. 1 The crystal structure and binding pocket of SARS-CoV-2 main protease (M^{Pro}) PDB: 6LU7 in complex with N3 native ligand (Jin et al. 2020)

Molecular docking simulation

AutoDock/Vina tool (Trott and Olson 2010) was used for the docking simulation. It is a reliable protein–ligand docking tool that uses the Broyden-Fletcher-Goldfarb-Shanno algorithm which significantly improves the average accuracy of the binding mode prediction (Azam and Abbasi 2013). AutoDock tool was used to generate the (.pdbqt) files using the grid size 58, 62, and 40 for x, y, and z axes, grid center $-26.284 \times 12.603 \times 58.960$ respectively, and 1.000 Å spacing. The docking simulation was performed using AutoDock

Fig. 2 The Ramachandran plot of SARS-CoV-2 main protease (M^{Pro}) PDB: 6LU7 VADAR (Volume, Area, Dihedral Angle Reporter) web-server



Vina and the binding energies (ΔG) (kcal/mol) of the docked ligands were obtained. The inhibition constants and inhibitory efficiencies of the docked ligands were calculated using (Eqs. 1 and 2). PyMol and Biovia-2019 discovery studio were used to view and analyse the docking results.

$$\Delta G = -RT \ln K_i \quad (1)$$

$$K_i = e^{\left[\frac{-\Delta G}{RT}\right]} \quad (2)$$

where R = Gas constant (1.987×10^{-3} kcal/mol); T = 298.15 K (absolute temperature); K_i = Inhibition constant; ΔG = Binding energy.

Prediction of activity spectra for substances (PASS) of the ligands

Prediction of Activity Spectra for Substances (PASS) web server <http://www.pharmaexpert.ru/passonline/> (Lagunin 2000) was used to predict the biological activities of the studied ligands.

Assessment of ADMET and drug-like properties

Absorption, distribution, metabolism, excretion and toxicity (ADMET) properties of the selected compounds were predicted using ADMET SAR2 web-server, while drug-like

features were evaluated using Molinspiration online tool (<http://molinspiration.com/>).

Results and discussion

Structural and active site analysis of SARS-CoV-2 M^{PRO} complexed with N3 inhibitor (PDB ID: 6LU7)

The X-ray crystallographic structure of SARS-CoV-2 M^{PRO} (PDB ID: 6LU7) (Fig. 1) contains 306 amino acid residues complexed with an inhibitor (N3-(N-[(5-Methylisoxazol-3-Yl)Carbonyl]Alanyl-L-Valyl-N~1~-(1r,2z)-4-(Benzyloxy)-4-Oxo-1-[(3r)-2-Oxopyrrolidin-3-Yl] Methyl)But-2-Enyl)-L-Leucinamide). It consists of 23%, 31%, 45% and 28% α -helix, β -sheets, Coil and Turns respectively. The resolution of the protease as revealed by X-ray diffraction was 2.16 Å, crystal dimension is a = 97.93 Å, b = 79.48 Å, and c = 51.08 Å with angles α (900), β (114.550), and γ (900) respectively. R-values (free, work, and observed) are 0.235, 0.202, and 0.204 respectively, while the Total Accessible Surface Area (TASA) on the protease is 14043.1 (Å²). There are three (3) domains which are: Domain I (residues 8–110), Domain II (residues 102–184), and Domain III (residues 185–200).

SARS-CoV-2 M^{PRO} active site is located in the cleft between Domain I and II and contains a Cys-His catalytic dyad. Amino acid residue at the active site is as follows Thr24, Thr25, Thr26, His41, Met49, Tyr54, Phe140, Leu141, Asn142, Gly143, Ser144, Cys145, His163, His164, Met165, Glu166, Leu176, Pro168, His172, Asp187, Arg188, Gln189, Thr190, Ala191, and Gln192 (Jin et al. 2020).

Molecular docking analysis

Recent developments in drug discovery have led to a renewed interest in the computational study which involves the use of algorithms and programs for predictions of therapeutic interventions in biological processes (Shoichet et al. 2002). Molecular Docking is a structure-based drug design approach that predicts binding interactions between ligand and target receptor at the binding site (Ferreira et al. 2015). It is an important virtual screening technique that could screen several thousands of ligands against the target as well as identify potential inhibitors of the target receptor with speed and accuracy (Dias et al. 2008).

To investigate potential inhibitors of SARS-CoV-2 M^{PRO}, AutoDock/Vina (MGL tools- 1.5.6), PyMOL Console Edu, and Biovia Discovery studio 4.5 were used. The results obtained from the docking of selected saponins and tannins against SARS-CoV-2 M^{PRO} were as shown in

Table 2 Binding Affinities and inhibition constant of selected Saponins and Tannins

S/N	Ligands	Binding affinity (ΔG) kcal/mol	Inhibition constant (K_i), μM
Saponins			
1	Priverogenin A	– 8.3	0.83
2	Arjunic acid	– 8.1	1.16
3	Theasapogenol B	– 8.1	1.16
4	Euscaphic Acid	– 8.0	1.37
5	Camelliagenin C	– 7.8	1.93
6	Medicagenic Acid	– 7.8	1.93
7	Protoescigenin	– 7.8	1.93
8	Arjunolic acid	– 7.7	2.28
9	Asiatic acid	– 7.7	2.28
10	Protobassic acid	– 7.7	2.28
11	Arjugenin	– 7.6	2.7
12	Primulagenin A	– 7.6	2.7
13	Soyasapogenol B	– 7.6	2.7
14	Tomentosic acid	– 7.6	2.7
15	Presenegenin	– 7.1	6.28
Tannins			
1	Punicalagin	– 9.0	0.25
2	Punicalin	– 8.6	0.5
3	Ellagic acid	– 8.4	0.7
4	Corilagin	– 8.2	0.98
5	Gallagic acid	– 8.1	1.16
6	Terflavin B	– 7.6	2.7
7	Catechin	– 7.5	3.2
8	Chebulinic acid	– 7.5	3.2
9	Hexahydroxy-diphenic acid	– 6.4	20.45
10	Gallic acid	– 5.5	93.34
11	Catechol	– 4.7	359.95
Standard (S) (SD)			
1	Remdesivir (SD-1)	– 7.6	2.7
2	Dexamethasone (SD-2)	– 7.7	2.28
3	N3Inhibitor (SD-3)	– 5.6	78.85

Table 2. Binding affinity is a reflection of the inhibitory activity of the plant extract against SARS-CoV-2 M^{PRO}. It is apparent from this table that most of the selected saponins and tannins had better binding affinities and inhibitory activities against SARS-CoV-2 M^{PRO} compared to Remdesivir and Dexamethasone which are standard drugs used in the management of this pandemic disease. Binding affinity (BA) for the selected saponins range between – 8.3 kcal/mol and – 7.1 kcal/mol, while those of tannins

range between -9.0 kcal/mol and -4.7 kcal/mol. It can be seen that selected tannins had far greater binding affinities compared to saponins, with Punicalagin (-9.0 kcal/mol) having the outstanding inhibitory activity. To validate the inhibitory effects observed through docking scores, the hit compounds among the docked ligands were subjected for further analysis.

ADMET assay of the selected hit compounds

Absorption, Distribution, Metabolism, Excretion, and Toxicity (ADMET) profile of a molecule is an important assay in the early stage of drug discovery. ADMET data enhances the selection and identification of molecules with optimum safety profile at a therapeutic dose along the discovery process rather than at the final stage, as this helps in avoiding waste of time and precious resources on drug molecules that may eventually be discarded (Tsaion and Kates 2010). Considering the binding affinities and inhibition constants (Table 2) which are expected to be within ($0.1 \mu\text{M}$ and $1.0 \mu\text{M}$), only nine (9) of the docked compounds qualified as hits and were subjected to ADMET analysis using ADMET SAR-2 web-server (Cheng et al. 2012). Notably, only Ellagic acid, Arjunic Acid, Thesapogenol B, and Euscaphic Acid

(coded C-1, C-2, C-3, and C-4 respectively) showed excellent ADMET profile, their structures were shown in Fig. 3, their ADMET properties were discussed in Table 3 and they were selected for further analyses. Although Punicalagin, Punicalin, and Priverogenin A had better inhibitory activities and binding affinities than ellagic acid, they were shunned on the basis of toxicity and the possibility of poor absorption and permeability across a biological membrane.

As part of the drug ADMET profile, a drug molecule should have good human intestinal absorption (HIA), solubility (Log S) range between -1 and -5 , should be a non-inhibitor of cytochrome P450 enzymes, and should be non-Ames toxic. Others include non-carcinogenicity, non-inhibition of hERG, and no or low level of toxicity (Tsaion and Kates 2010). C-1, C-2, C-3, and C-4 (Table 3) were well absorbed in the human intestine, only Thesapogenol B (C-3) was found to cross the blood–brain barrier, although an oral drug does not necessarily need to cross the blood–brain barrier, only central nervous system target drug need to (Hughes et al. 2011).

It was also found in the prediction, that all the four (4) selected hit compounds were non-inhibitor of microsomal enzymes (Cytochrome P450), which is an indication of good metabolism of the drug in the liver (Stevens 2014).

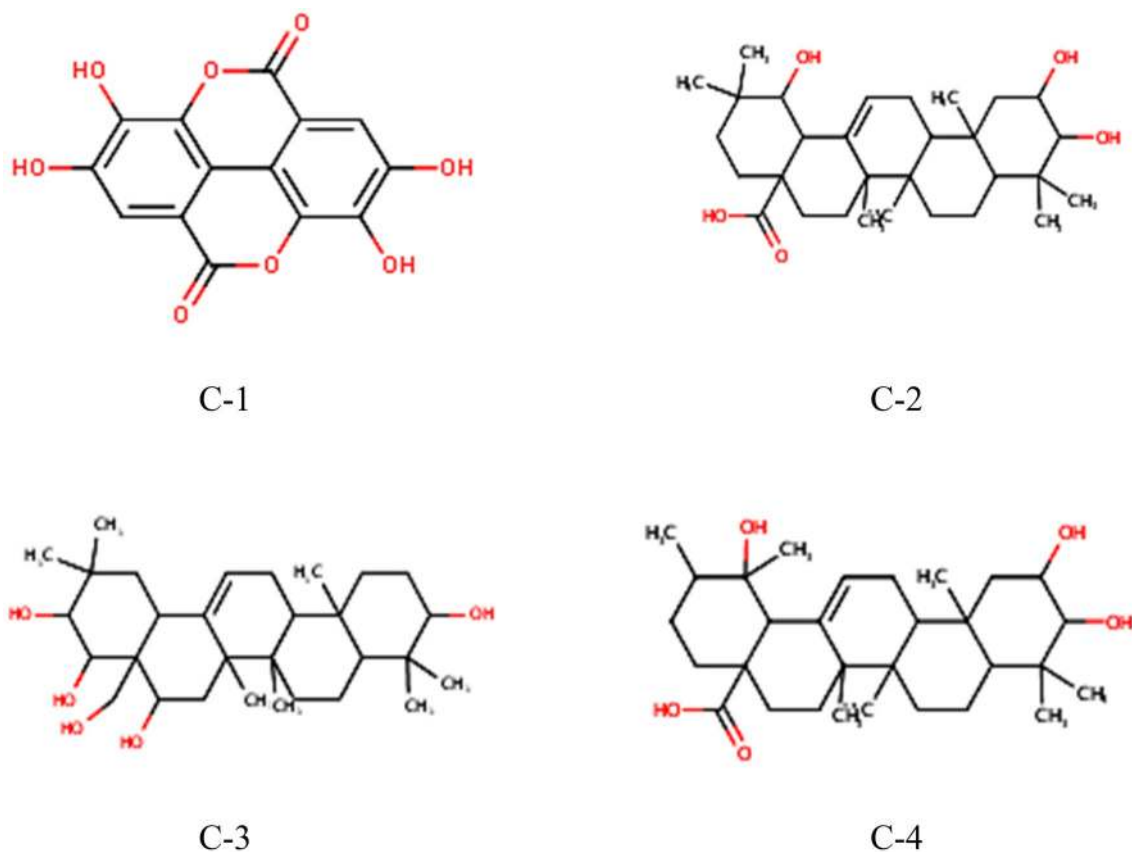


Fig. 3 The 2D Structures of selected hit compounds C-1=Ellagic Acid; C-2=Arjunic Acid; C-3=Thesapogenol B; C-4=Euscaphic Acid

Table 3 ADMET prediction of selected compounds

Absorption and Distribution	C-1	C-2	C-3	C-4	SD-1	SD-2	SD-3
BBB (\pm)	0.6372 (BBB $-$)	0.3145 (BBB $-$)	0.8187 (BBB $+$)	0.5278 (BBB $-$)	0.9625 (BBB $+$)	1.0000 (BBB $+$)	0.9499 (BBB $+$)
HIA $+$	98.15%	96.43%	97.21%	97.46%	91.35%	99.3%	91.8%
Aqueous Solubility (LogS)	- 3.144	- 4.446	- 3.753	- 4.129	- 3.474	- 3.703	- 3.068
Metabolism							
CYP450 2C19 Inhibitor	0.8017 Non-Inhibitor	0.8826 Non-Inhibitor	0.8633 Non-Inhibitor	0.8799 Non-Inhibitor	0.7362 Non-Inhibitor	0.9247 Non-Inhibitor	0.7512 Non-Inhibitor
CYP450 1A2 Inhibitor	0.5914 Non-Inhibitor	0.8863 Non-Inhibitor	0.8936 Non-Inhibitor	0.7582 Non-Inhibitor	0.7447 Non-Inhibitor	0.9380 Non-Inhibitor	0.8546 Non-Inhibitor
CYP450 3A4 Inhibitor	0.9078 Non-Inhibitor	0.8734 Non-Inhibitor	0.8723 Non-Inhibitor	0.7415 Non-Inhibitor	0.7224 Non-Inhibitor	0.8308 Non-Inhibitor	0.5508 Non-Inhibitor
CYP450 2C9 Inhibitor	0.5591 Non-Inhibitor	0.8938 Non-Inhibitor	0.8595 Non-Inhibitor	0.8493 Non-Inhibitor	0.7246 Non-Inhibitor	0.9106 Non-Inhibitor	0.7871 Non-Inhibitor
CYP450 2D6 Inhibitor	0.9575 Non-Inhibitor	0.9476 Non-Inhibitor	0.9368 Non-Inhibitor	0.9607 Non-Inhibitor	0.8503 Non-Inhibitor	0.9231 Non-Inhibitor	0.8689 Non-Inhibitor
Excretion							
Biodegradation	0.8250 Not biodegradable	0.8500 Not biodegradable	0.9250 Not biodegradable	0.8250 Not biodegradable	0.7750 Not biodegradable	0.8750 Not biodegradable	0.7750 Not biodegradable
Toxicity							
AMES	0.8200	0.9000	0.8600	0.8600	0.7400	0.6300	0.6700
Mutagenesis	Non-Ames Toxic	Non-Ames Toxic	Non-Ames Toxic	Non-Ames Toxic	Non-Ames Toxic	Non-Ames Toxic	Non-Ames Toxic
Acute Oral Toxicity	0.6020 III	0.6470 III	0.7710 III	0.7326 III	0.5357 III	0.8328 III	0.6034 III
Eye irritation (YES/NO)	YES	NO	NO	NO	NO	NO	NO
Eye corrosion (YES/NO)	NO	NO	NO	NO	NO	NO	NO
hERG inhibition	0.8048 NO	0.5631 NO	0.4360 NO	0.5439 NO	0.5000 NO	0.6942 YES	0.6806 YES
Carcinogenicity	1.0000 Non-Carcinogenic	1.0000 Non-Carcinogenic	0.9857 Non-Carcinogenic	0.9286 Non-Carcinogenic	0.9714 Non-Carcinogenic	0.9286 Non-Carcinogenic	0.7857 Non-Carcinogenic

C-1 = Ellagic Acid; C-2 = Arjunic Acid; C-3 = Thesapogenol B; C-4 = Euscaphic Acid; SD-1 = Remdesivir; SD-2 = Dexamethasone, SD-3 = N3 inhibitor

The potential of a drug molecule to cause mutation in DNA is revealed by Ames toxicity value and could be a major reason for excluding a drug molecule along the discovery process (Mccarren et al. 2011). As shown in Table 3, all the selected hit compounds are non-genotoxic and non-carcinogenic. Similarly, the hits possess type III acute oral toxicity values (slightly toxic) which could easily be converted to type IV (nontoxic) during hit-lead optimization. The human ether-a-go-go related gene (hERG) potassium ion channel plays important role in cardiac repolarization, blockage of which may be caused by inherited mutation or some drug molecules, leading to long QT syndrome and eventual death (Sanguinetti and Tristani-firouzi 2006). Interestingly all the hit compounds are non-blockers of the hERG potassium channel.

Comparison of ADMET profile of the hits with the standard drugs revealed that Remdesivir, Dexamethasone, and N3 inhibitor had good ADMET profiles, but both dexamethasone and N3 inhibitor were found to be blockers of hERG potassium ion channel while Remdesivir is not. This result, therefore, suggests that the hit compounds have a similar ADMET profile just like Remdesivir, and could be developed further in the quest of finding a new therapeutic agent in COVID-19 management. It is important to note that the ADMET profile of dexamethasone revealed that it is a blocker of hERG potassium ion channel, therefore caution should be taken in its administration to COVID-19 patients.

Drug-like analysis of the selected compounds

Evaluation of physicochemical and drug-likeness of the potential active compound is an important step in drug discovery. As proposed by Lipinski, an effective oral therapeutic drug must obey the ‘rule of five’ with not more than one (1) violation, this is due to the fact that an orally bioavailable drug must possess molecular weight (MW) ≤ 500 Da, hydrogen bond donor (HBDs) ≤ 5 , hydrogen bond acceptor (HBAs) ≤ 10 and log P (octanol–water partition coefficient) ≤ 5 (Lipinski 2004). These descriptors of oral bioavailability are important as they predict the permeability and absorption of such drug across a biological membrane such as an epithelium cell, partition coefficient value (log p) is especially important in predicting intestinal absorption of such drug (Aucamp et al. 2015). Drug-likeness of the selected hits were evaluated with Molinspiration online

(<http://www.molinspiration.com/>) as shown in Table 4, it is apparent from the table that none of the selected hits had more than one violation of the ‘rule of five’ which is an indication of good oral bioavailability and permeability. It is also interesting to note that all the selected hits and Dexamethasone (SD-2) had better drug-like properties compared to Remdesivir, and N3-Inhibitor (SD-1 and SD-3) with more than 1 violation. This result revealed that the selected hits (C-1 to C-4) possessed excellent drug-like properties and could be developed further as oral drugs.

Oral-bioavailability of the selected hit compounds and standards

Table 5 shows the oral-bioavailability profile of the selected hit ligands and standards obtained using the swissADME tool (Daina et al. 2017). The bioavailability radar (Fig. 4) revealed

Table 4 Drug-likeness of selected hit compounds

Compounds	Heavy atoms (HA)	Molecular Weight (MW)	RO5 violations	Hydrogen bond donor (HBD)	Hydrogen bond acceptor (HBA)	miLog P
C-1	22	302.19	0	4	8	0.94
C-2	35	488.71	0	4	5	4.89
C-3	35	490.73	0	5	5	4.10
C-4	35	488.71	0	4	5	4.93
SD-1	42	602.59	2	5	14	2.82
SD-2	28	392.47	0	3	5	2.06
SD-3	49	680.80	2	5	14	2.32

C-1 = Ellagic Acid, C-2 = Arjunic Acid, C-3 = Theasapogenol B, C-4 = Euscaphic Acid, SD-1 = Remdesivir, SD-2 = Dexamethasone, SD-3 = N3 Inhibitor

Table 5 Oral bioavailability of the selected hit compounds

LIGAND	C-1	C-2	C-3	C-4	SD-1	SD-2	SD-3
Formula	C ₁₄ H ₆ O ₈	C ₃₀ H ₄₈ O ₅	C ₃₀ H ₅₀ O ₅	C ₃₀ H ₄₈ O ₅	C ₂₇ H ₃₅ N ₆ O ₈ P	C ₂₂ H ₂₉ FO ₅	C ₃₅ H ₄₈ N ₆ O ₈
VINA Score	- 8.4	- 8.1	- 8.1	- 8.0	- 7.6	- 7.7	- 5.6
Mass	302.19	488.7	490.7	488.7	602.6	392.5	680.79
TPSA	141.34	97.99	101.15	97.99	213.36	94.83	197.83
#Rotatable bonds	0	1	1	1	14	2	22
XLOGP3	1.10	5.17	4.64	4.96	1.91	1.94	3.35
WLOGP	1.31	5.18	4.05	5.18	2.21	2.32	1.55
ESOL Log S	- 2.94	- 6.06	- 5.74	- 5.93	- 4.12	- 3.36	- 4.89
ESOL CLASS	Soluble	Poorly soluble	Moderately soluble	Moderately soluble	Moderately soluble	Soluble	Moderately soluble
Lipinski #violations	0	0	0	0	2	0	2
Bioavailability Score	0.55	0.56	0.55	0.556	0.17	0.55	0.17
PAIN #alerts	1	0	0	0	0	0	0
Fraction Csp3	0.00	0.90	0.93	0.90	0.48	0.73	0.51
Synthetic Accessibility	3.17	6.53	6.72	6.59	6.33	5.47	6.43

C-1 = Ellagic, C-2 = Arjunic acid, C-3 = Theasapogenol B, C-4 = Euscaphic acid SD-1 = Remdesivir, SD-2 = Dexamethasone, SD-3 = N3 Inhibitor

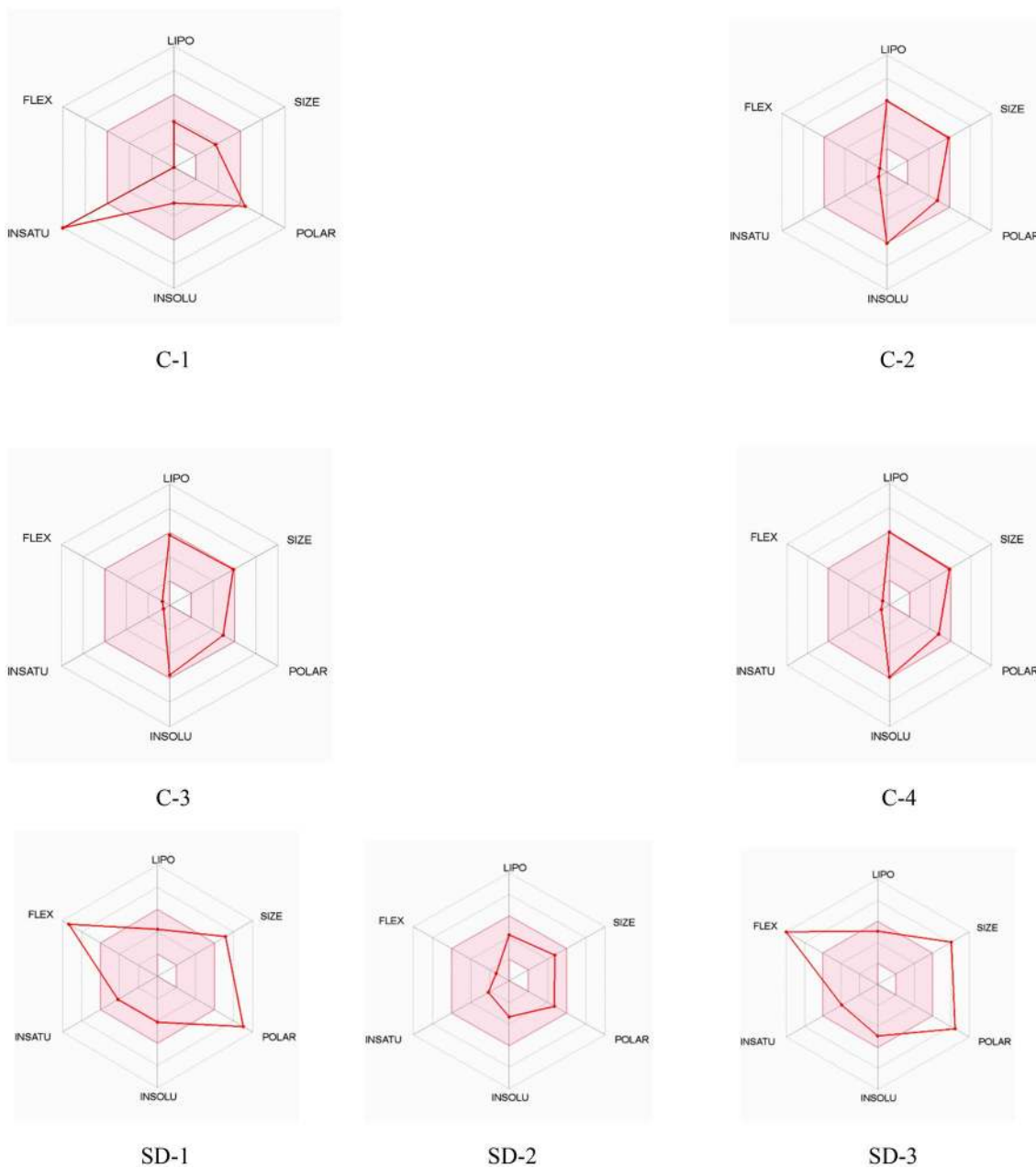


Fig. 4 The bioavailability radar for the selected hit compounds and Standards (C-1) Ellargic acid; (C-2) Arjunic acid; (C-3) Theasapogenol B; (C-4) Euscaphic acid; (SD-1) Remdesivir; (SD-2) Dexamethasone, and (SD-3) N3-Inhibitor

the oral-bioavailability profile of the selected hits and Standard drug in a catch sight. The pink area of the radar shows the optimum zone for each of the properties i.e., (POLAR, FLEX, SIZE LIPO, INSATU, and INSOLU). As shown in Table 5, all the selected hits obeyed the recommended size of 500 gmol⁻¹ for effective drug candidates as reported by Lipinski, compared to 602.6 gmol⁻¹ and 680.79 gmol⁻¹ reported for SD-1 and SD-3 respectively. The polarity (POLAR) of the selected hits were evaluated using their Total Polarity Surface Area (TPSA). A polar compound is expected to have TPSA

value within the range of 20 and 130 Å². The TPSA of C-2 and C-3 fall within the recommended range, while all the hit compounds have lower TPSA values compared to the value obtained for SD-1 and SD-3. However, SD-2 has the best TPSA value (94Å²), thus has the highest POLARITY property. The INSOLU (insolubility) requirement of the selected compounds and standards as depicted in their ESOL (Log S) and ESOL Class showed that C-1 and SD-2 are soluble; C-2 has a poor solubility profile while C-3, C-4, SD-1, and SD-3 are moderately soluble. Notably, C-1 has the most outstanding

ESOL (Log S) (− 2.94) and the highest aqueous solubility property among the selected hit compounds and standards. The fraction of carbon Sp3 (CSP3) and the number of the rotatable bond are expected to be within the range of 0.5–1 (CSP3) and should not exceed nine (#Rotatable bonds). They are used to evaluate the unsaturation (INSATU) and flexibility (FLEX) of the selected hits and standards. Interestingly, all the selected hits and Standards had CSP3 values within the recommended range. The numbers of rotatable bonds in all the selected hits do not exceed nine (9) as compared to SD-1 and SD-3 with 14 and 22 respectively. xLogP3 and ESOL (Log S) with the recommended range of (− 0.7 and + 5.0), and (0 and 6) respectively were used to access the Lipophilicity (LIPO) and Insolubility (INSOLU) profile of the selected hits and standards. Except for C-2, the xLogP3 and ESOL (Log S) of all the selected hits and standards fall within the recommended range. Put together, all the selected hits and standards are orally available and could be explored further in the quest of finding a new therapeutic agent for COVID-19 management.

Bioactivity of the selected compounds

Table 6 shows the bioactivity properties of the four (4) selected hits and standards. The inverse relationship existing between binding energy and inhibition constant is as shown in Eqs. 1 and 2, indicating that the higher the binding energy the lower the inhibition constant. A potential hit compound is expected to have inhibition constant values ranging between 0.1 and 1.0 μM and not more than 10 nM for a drug (Stevens 2014). Inhibition constant values of the hit compounds range from 0.70 to 1.37 μM. This observation revealed that all the four (4) selected compounds are qualified as hit with Ellagic acid (0.70 μM) being the most potent of all. Ligand Efficiency (LE), Fit Quality (FQ), and Ligand-efficiency-dependent lipophilicity (LELP) were also calculated according to Eq. 3–6. C-1 has the ligand efficiency (LE) value within the recommended value of (≥ 0.3), while both C-1 and SD-2 have LELP values within the recommended range of (− 10 and 10). Notably, all the hit compounds had FQ values within the recommended

range (≥ 0.8), which is higher than the FQ values reported for all the standards (Hopkins et al. 2014).

$$\text{Ligand Efficiency (LE)} = -B.E \div \text{Heavyatoms (H.A)} \quad (3)$$

$$LE_{scale} = 0.873e^{-0.026 \times H.A} - 0.064 \quad (4)$$

$$FQ = LE \div LE_{scale} \quad (5)$$

$$ELP = \text{LogP} \div LE. \quad (6)$$

Prediction of activity spectra for substances (PASS) biological activity prediction of selected compounds and standards

Table 7 shows the prediction of the biological activity spectra of the selected hits and standards using the PASS online web tool (Filimonov et al. 2014). It shows predictions based on the structure–activity relationship (SAR). Pa is the probability that shows the similarity in structure of specific molecules in comparison to the molecules of the most active compound of similar activity. For this activity spectrum, the probability of validating the biological activity of a molecule

Table 7 Prediction of activity spectra for the selected hit compounds

Ligands	Probability to be Active Pa	Probability to be Inactive Pb	Biological activities
Ellagic acid	0.322	0.029	Antiviral
Arjunic acid	0.169	0.136	Antiviral
Theasapogenol B	0.257	0.056	Antiviral
Euscaphic acid	0.286	0.042	Antiviral
Remdesivir	0.814	0.004	Antiviral
Dexamethasone	–	–	–
Inhibitor N3	0.698 0.665	0.001 0.002	Severe acute respiratory syndrome treatment Protease Inhibitor

Table 6 Bioactivity analysis of the selected hit compounds and standards

Bioactivity	C-1	C-2	C-3	C-4	SD-1	SD-2	SD-3
AutoDock Vina docking score (kcal/mol)	− 8.40	− 8.10	− 8.10	− 8.00	− 7.6	− 7.7	− 5.6
Ki (μM)	0.70	1.16	1.16	1.37	2.70	2.28	78.85
miLog P	0.94	4.89	4.10	4.80	2.82	2.06	2.32
Ligand efficiency (LE) /kcal/mol/heavy atom)	0.38	0.23	0.23	0.23	0.18	0.28	0.11
LE-scale	0.43	0.29	0.29	0.29	0.23	0.36	0.18
Fit quality (FQ)	0.89	0.81	0.81	0.80	0.79	0.77	0.63
Ligand-efficiency-dependent lipophilicity (LELP)	2.47	21.13	17.72	21.00	15.58	7.49	20.30

C-1 = Ellagic acid; C-2 = Arjunic acid; C-3 = Theasapogenol B; C-4 = Euscaphic acid; SD-1 = Remdesivir; SD-2 = Dexamethasone; SD-3 = Inhibitor N3

experimentally must increase with higher values of Pa and lower values of Pi i.e., $p_a > p_i$ (Filimonov et al. 2014). It can be observed from Table 7 that all the selected hits (Ellagic acid, Arjunic acid, Theasapogenol, and Euscaphic acid) and SD-1 (Remdesivir) possess antiviral activities while (SD-2) Dexamethasone showed no antiviral activity within the spectrum. Also, Table 7 revealed that SD-3 had higher activity spectra for severe acute respiratory syndrome treatment and Protease Inhibition potential with Pa values of 0.698 and 0.665 respectively, which is an indication of its tendency to inhibit the SARS CoV-2 main protease. Notably, The Pa values observed for the hit compounds were greater than Pi, thus validating their biological activities. Therefore, all the selected hits possessed excellent antiviral activities and could be explored in the design and development of new drugs/vaccines in the management of the novel SARS-CoV-2 ravaging the globe.

Binding mode and molecular interactions of the selected hits and standards

Identifying the binding site and evaluating the binding interactions of the ligands in the active pocket of the target receptor plays a crucial role in drug design. This eases the improvement of ligand affinity to the pocket during the lead optimization stage of drug discovery. The binding interactions of the selected hits and standards with SARS-CoV-2 main protease (M^{pro}) are shown in Tables 8 and 9. The binding affinities obtained from the docking of C-1, C-2, C-3, C-4, SD-1, and SD-2 as shown in Table 8 are (− 8.4, − 8.1, − 8.1, − 8.0, − 7.6, and − 7.7 kcal/mol) respectively. C-1 (Table 9) formed a conventional hydrogen bond with Gln189, Leu141, Gly143, Ser144, His163, and Asn142, carbon-hydrogen bond with His172, pi-donor hydrogen bond with Met165, pi-alkyl interaction with Cys145. However, a close examination of the main active site of the target receptor (6LU7) revealed that its binding pocket (active site) was located in the cleft between domains I and II with

Cysteine and Histidine residues forming catalytic dyad in its active site (Jin et al. 2020). Interestingly, All the amino acids reported above for C-1 (Table 9) are also found in the active site of the target receptor (6LU7) (see Sect. “Structural and Active site analysis of SARS-CoV-2 Mpro complexed with N3 inhibitor (PDB ID: 6LU7)”). This implies that C-1 shares the same pocket and interacts effectively with the active site of the target receptor and could be its potential inhibitor.

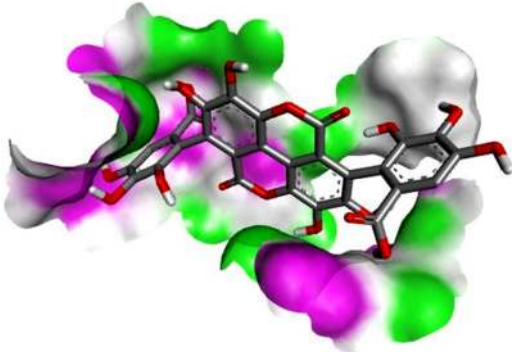
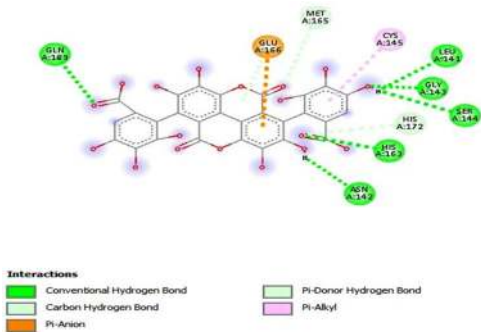
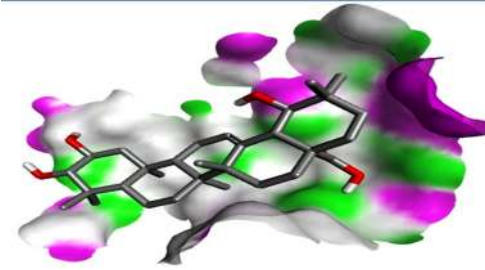
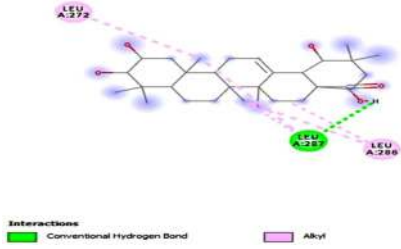
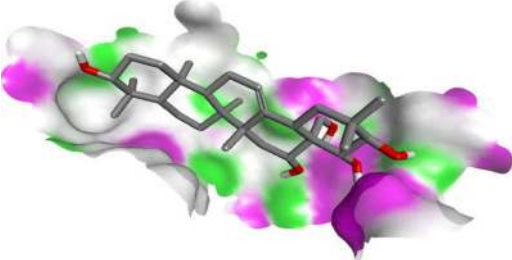
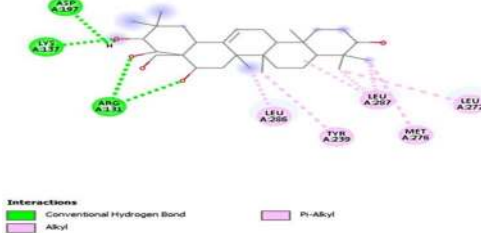
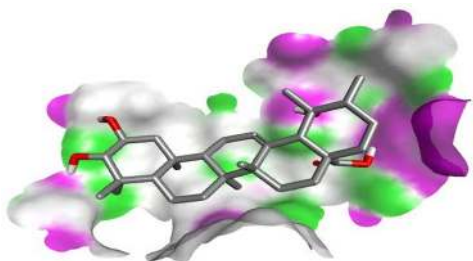
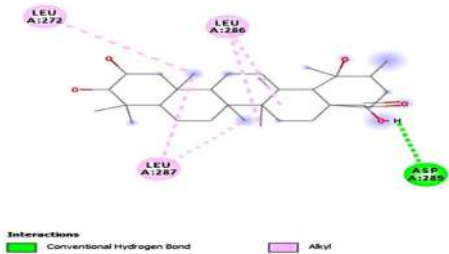
Furthermore, strong similarities were observed in the interactions of C-2, C-3, and C-4 with 6LU7 (Table 9) as compared with standards SD-1 and SD-2 (Table 8). C-2 formed a conventional hydrogen bond with Leu287, and alkyl interaction with Leu286; C-3 formed a conventional hydrogen bond with Asp197, Arg131, and Lys137, alkyl and pi-alkyl interactions with Leu286, Tyr239, Leu287, Met276, and Leu272; C-4 formed a conventional hydrogen bond with Asp289, and alkyl interactions with Leu287, Leu273, and Leu286. Obviously, Leu286 and Leu287 (Table 9) are common to C-2, C-3, and C-4. This affirmed the similarity in their pocket and interactions. Notably, Leu286 and Leu287 common to C-2, C-3, and C-4 were also found in SD-1 and SD-2 (Table 8). Therefore, C-2, C-3, and C-4 shared the same pocket and interactions with SD-1 and SD-2. However, the pocket shared between these hits and the standards are not the active site of the target receptor (Jin et al. 2020), although, it has been reported that the adjoining binding pockets to the active site may also be employed in the designing of therapeutic agent (Anand et al. 2002). Also, SD-1 (Remdesivir) and SD-2 (Dexamethasone) share the same pocket with C-2, C-3 and.

C-4 have completed their randomized clinical trials as potential inhibitors of 6LU7 (Kaddoura et al. 2020), suggesting that they are allosteric inhibitors.

Table 8 Docking scores, binding sites and inhibition constants of the selected hit compounds and standards with SARS-CoV-2 main protease (M^{pro})

Ligands	Binding Affinity (ΔG), kcal/mol	6LU7 Receptor amino acids forming H-bond with ligands	Electrostatic/Hydrophobic Interactions involved	Inhibition constant (K_i), μM
Remdesivir	− 7.6	Lys13, Asp289, Thr199, Leu287	Tyr237, Asn238	2.28
Dexamethasone	− 7.7	Lys137, Asp289, Asp289, Thr199, Leu287, Leu271	Leu286	2.70
Ellagic acid	− 8.4	Gln189, Leu141, Asn142, His163, Ser144, Gly143	Glu166, Met165, Cys145, His172	0.25
Arjunic acid	− 8.1	Leu287	Leu286	1.16
Theasapogenol B	− 8.1	Lys137, Asp197, Arg131	Tyr239, Leu272, Met276, Leu286, Leu287	1.16
Euscaphic Acid	− 8.0	Asp289	Leu273, Leu286, Leu287	1.37

Table 9 Binding mode and molecular interactions of the selected hits against 6LU7

Ligands	Binding pockets	Interactions
C-1		
C-2		
C-3		
C-4		

C-1 = Ellagic acid; C-2 = Arjunic acid; C-3 = Theasapogenol B; C-4 = Euscaphic acid

Conclusion

This study evaluates twenty-seven (27) bioactive saponins/tannins against SARS-CoV-2 main protease (M^{pro}) via in silico studies (structure-based drug design). The compounds were screened using the reliable AutoDock/Vina tool, ADMET SAR-2, swissADME, Molinspiration web server, PASS software, among others. CASTp and VADAR web tools were used to establish the active site and Ramachandran plot of the target receptor (6LU7) respectively. The

results obtained flourish Ellagic acid (– 8.4 kcal/mol), Arjunic acid (– 8.1 kcal/mol), Theasapogenol B (– 8.1 kcal/mol), and Euscaphic Acid (– 8.0 kcal/mol) as probable inhibitors of SARS-CoV-2 M^{pro} due to their excellent binding energies, ADMET profile, drug-likeness, oral-bioavailability properties, PASS properties, Bioactivity, outstanding binding mode and molecular interactions with the target receptor. C-1 (Ellagic acid) share the same pocket and interact completely with the active site of the target receptor, while C-2, C-3, and C-4 (Arjunic acid, Theasapogenol B, Euscaphic

Acid) respectively share the same probable allosteric pocket and interactions with SD-1 (Remdesivir), and SD-2 (Dexamethasone) whose randomized clinical trials against the target receptor have been completed. Although, it is widely accepted that computational drug-design plays a pivotal role in the world of drug design and development today. It is used in hit/lead identification and optimization towards the design and development of new therapeutic agents, however, the need for experimental work to buttress our findings is duly acknowledged, but lack of funding among other factors limited our scope. We hereby recommend that the four-hit compounds identified in this study should be developed further towards finding a reliable and effective drug/vaccine to arrest the new disease (COVID-19) terrorizing the entire human race.

Acknowledgements The authors wish to acknowledge members of the Computational and Biophysical Chemistry Research Group in the Department of Pure and Applied Chemistry, Ladoke Akintola University of Technology, LAUTECH, Ogbomoso, Oyo State, Nigeria.

Author contributions MA-H, ATI: conceptualization, methodology, validation, supervision, writing-review and editing, visualization, data curation, resources. VAF and IOA: conceptualization, writing—original draft, writing-review and editing, methodology, investigation, data curation, visualization. TAL and SAA: conceptualization, methodology, data curation, investigation, visualization.

Funding The author(s) received no financial aid or support in any form for this research work.

Compliance with ethical standards

Conflict of interest The authors declare that there is no conflict of interest in this manuscript.

References

- Anand K, Palm GJ, Mesters JR et al (2002) Structure of coronavirus main proteinase reveals combination of a chymotrypsin fold with an extra alpha-helical domain. *EMBO J* 21:3213–3224
- Aucamp M, Odendaal R, Liebenberg W, Hamman J (2015) Amorphous azithromycin with improved aqueous solubility and intestinal membrane permeability. *Drug Dev Ind Pharm* 41(7):1100–1108. <https://doi.org/10.3109/03639045.2014.931967>
- Azam SS, Abbasi SW (2013) Molecular docking studies for the identification of novel melatoninergic inhibitors for acetylserotonin-*O*-methyltransferase using different docking routines. *Theor Biol Med Model*. <https://doi.org/10.1186/1742-4682-10-63>
- Chang L, Yan Y, Wang L (2020) Coronavirus disease 2019: coronaviruses and blood safety. *Transfus Med Rev* 34(2):75–80. <https://doi.org/10.1016/j.tmr.2020.02.003>
- Chen N, Zhou M, Dong X et al (2020) Epidemiological and clinical characteristics of 99 cases of 2019 novel coronavirus pneumonia in Wuhan, China: a descriptive study. *Lancet* 395:507–513. [https://doi.org/10.1016/S0140-6736\(20\)30211-7](https://doi.org/10.1016/S0140-6736(20)30211-7)
- Cheng F, Li W, Zhou Y et al (2012) admetSAR: a comprehensive source and free tool for assessment of chemical ADMET properties. *J Chem Inf Model* 52(11):3099–3105. <https://doi.org/10.1021/ci300367a>
- Daina A, Michielin O, Zoete V (2017) SwissADME: a free web tool to evaluate pharmacokinetics, drug-likeness and medicinal chemistry friendliness of small molecules. *Sci Rep* 7:42717. <https://doi.org/10.1038/srep42717>
- Dias R, Filgueira W, Jr DA (2008) Molecular docking algorithms. 9(12): 1040–1047. <https://doi.org/10.2174/138945008786949432>
- Ferreira LG, Santos RN, Oliva G, Andricopulo AD (2015) Molecular docking and structure-based drug design strategies. *Molecules* 20:13384–13421. <https://doi.org/10.3390/molecules200713384>
- Filimonov DA, Lagunin AA, Glorizova TA, Rudik AV et al (2014) Prediction of the biological activity spectra of organic compounds using the PASS online web resource. *Chem Heterocyclic Compounds, Russian Original* 50(3):444–457. <https://doi.org/10.1007/s10593-014-1496-1>
- Francis G, Kerem Z, Makkar HPS, Becker K (2002) The biological action of saponins in animal systems: a review. *Br J Nutr* 88(6):587–605. <https://doi.org/10.1079/BJN2002725>
- Guclu-Ustundag Ö, Mazza G (2007) Saponins: properties, applications and processing. *Crit Rev Food Sci Nutr* 47(3):231–258. <https://doi.org/10.1080/10408390600698197>
- Hajduk PJ, Huth JR, Tse C (2005) Predicting protein druggability. *Drug Discovery Today* 10:1675–1682. [https://doi.org/10.1016/S1359-6446\(05\)03624-X](https://doi.org/10.1016/S1359-6446(05)03624-X)
- Hopkins AL, Keserü GM, Leeson PD et al (2014) The role of ligand efficiency metrics in drug discovery. *Nat Rev Drug Discov* 13(2):105–121. <https://doi.org/10.1038/nrd4163>
- Hughes JP, Rees S, Kalindjian SB, Philpott KL (2011) Principles of early drug. *Br J Pharmacol* 162:1239–1249. <https://doi.org/10.1111/j.1476-5381.2010.01127.x>
- Jin Z, Du X, Xu Y et al (2020) Structure of Mpro from COVID-19 virus and discovery of its inhibitors. *Nature* 582:289–293. <https://doi.org/10.1038/s41586-020-2223-y>
- Johnson RM, Vinetz JM (2020) Dexamethasone in the management of covid -19. *BMJ* 370:1–2. <https://doi.org/10.1136/bmj.m264>
- Kaddoura M, Albrahim M, Hijazi G, Soudani N, Audi A, Alkalamouni H, Haddad S, Eid A, Zaraket H (2020) COVID-19 therapeutic options under investigation. *Front Pharmacol* 11:1196. <https://doi.org/10.3389/fphar.2020.01196>
- Lagunin A, Stepanchikova A, Filimonov D, Poroikov V (2000) PASS: prediction of activity spectra for biologically active substances. *Bioinformatics* 16(8):747–748. <https://doi.org/10.1093/bioinformatics/16.8.747>
- Lipinski CA (2004) Lead profiling Lead- and drug-like compounds: the rule-of-five revolution. *Drug Discov Today* 1(4):337–341. <https://doi.org/10.1016/j.ddtec.2004.11.007>
- Mccarren P, Springer C, Whitehead L (2011) An investigation into pharmaceutically relevant mutagenicity data and the influence on Ames predictive potential. *J Cheminform* 3(51):1–20. <https://doi.org/10.1186/1758-2946-3-51>
- Roner MR, Sprayberry J, Spinks M, Dhanji S (2007) Antiviral activity obtained from aqueous extracts of the Chilean soapbark tree (*Quillaja saponaria* Molina). *J Gen Virol* 88(1):275–285. <https://doi.org/10.1099/vir.0.82321-0>
- Sanguinetti MC, Tristani-firouzi M (2006) hERG potassium channels and cardiac arrhythmia. *Nature* 440:463–469. <https://doi.org/10.1038/nature04710>
- Serrano J, Puupponen-pimiä R, Dauer A, Aura A (2009) Review Tannins: current knowledge of food sources, intake, bioavailability and biological effects. *Mol Nutr Food Res*. <https://doi.org/10.1002/mnfr.200900039>

- Shoichet BK, McGovern SL, Wei B, Irwin JJ (2002) Lead discovery using molecular docking. *Curr Opin Chem Biol* 6:439–446. [https://doi.org/10.1016/s1367-5931\(02\)00339-3](https://doi.org/10.1016/s1367-5931(02)00339-3)
- Skene CD, Sutton P (2006) Saponin-adjuvanted particulate vaccines for clinical use. *Methods* 40(1):53–59. <https://doi.org/10.1016/j.ymeth.2006.05.019>
- Stevens E (2014) Lead Discovery. In: Jaworski A (ed) *Medicinal chemistry: modern drug discovery process*. Pearson, pp 247–272
- Sun H, Xie Y, Ye Y (2009) Advances in saponin-based adjuvants. *Vaccine* 27(12):1787–1796. <https://doi.org/10.1016/j.vaccine.2009.01.091>
- Tian W, Chen C, Lei X et al (2019) CASTp 3.0: computed atlas of surface topography of proteins. *Nucleic Acids Res* 46:W363–W367
- Trott O, Olson AJ (2010) Software news and update AutoDock Vina: improving the speed and accuracy of docking with a new scoring function, efficient optimization, and multithreading. *J Comput Chem* 31:455–461
- Tsaioun K, Kates SA (2010) *ADMET for medicinal chemists: a practical guide*. John Wiley and Sons, Singapore, pp 145–200. <https://doi.org/10.1002/9780470915110>
- Vincken J, Heng L, De GA, Gruppen H (2007) Saponins, classification and occurrence in the plant kingdom. *Phytochemistry* 68(3):275–297. <https://doi.org/10.1016/j.phytochem.2006.10.008>
- Wang M, Cao R, Zhang L et al (2020) Remdesivir and chloroquine effectively inhibit the recently emerged novel coronavirus (2019-nCoV) in vitro. *Cell Res* 30:269–271. <https://doi.org/10.1038/s41422-020-0282-0>
- Wu R, Wang L, Kuo HCD et al (2020) An update on current therapeutic drugs treating COVID-19. *Curr Pharmacol Rep*. <https://doi.org/10.1007/s40495-020-00216-7>
- Zhou P, Yang X, Wang X et al (2020) A pneumonia outbreak associated with a new coronavirus of probable bat origin. *Nature* 579:270–273. <https://doi.org/10.1038/s41586-020-2012-7>

Publisher's Note Springer Nature remains neutral with regard to jurisdictional claims in published maps and institutional affiliations.